Histone H4K20me3 and HP1α are late heterochromatin markers in development, but present in undifferentiated embryonic stem cells

Tuempong Wongtawan[1,2,3,*], Jane E. Taylor[1], Kirstie A. Lawson[4], Ian Wilmut[1] and Sari Pennings[2,*]

[1]MRC Centre for Regenerative Medicine, University of Edinburgh, 49 Little France Crescent, Edinburgh EH16 4SB, UK
[2]Centre for Cardiovascular Science, Queen's Medical Research Institute, University of Edinburgh, 47 Little France Crescent, Edinburgh EH16 4TJ, UK
[3]Faculty of Veterinary Science, Mahidol University, Salaya Nakhonpathom 73170, Thailand
[4]Human Genetics Unit, Medical Research Council, Crewe Road, Edinburgh EH4 2XU, UK
*Authors for correspondence (Tuempong.Wongtawan@ed.ac.uk; Sari.Pennings@ed.ac.uk)

Accepted 20 January 2011
Journal of Cell Science 124, 1878-1890

doi:10.1242/jcs.080721

Summary

We report here that the formation of heterochromatin in cell nuclei during mouse development is characterised by dynamic changes in the epigenetic modifications of histones. Our observations reveal that heterochromatin in mouse preimplantation embryos is in an immature state that lacks the constitutive heterochromatin markers histone H4 trimethyl Lys20 (H4K20me3) and chromobox homolog 5 (HP1α, also known as CBX5). Remarkably, these somatic heterochromatin hallmarks are not detectable – except in mural trophoblast – until mid-gestation, increasing in level during foetal development. Our results support a developmentally regulated connection between HP1α and H4K20me3. Whereas inner cell mass (ICM) and epiblast stain negative for H4K20me3 and HP1α, embryonic stem (ES) cell lines, by contrast, stain positive for these markers, indicating substantial chromatin divergence. We conclude that H4K20me3 and HP1α are late developmental epigenetic markers, and slow maturation of heterochromatin in tissues that develop from ICM is ectopically induced during ES cell derivation. Our findings suggest that H4K20me3 and HP1α are markers for cell type commitment that can be triggered by developmental or cell context, independently of the differentiation process.

Key words: ES cells, Development, Heterochromatin, Histone methylation

Introduction

Advances in histone modification mapping have revealed that different histone signatures are associated with various chromatin states. In accordance with a loosely defined histone code, prevalent combinations of modifications have been found to demarcate the substructures of active genes, as well as the global nuclear compartments of euchromatin and heterochromatin (Schones and Zhao, 2008). Heterochromatin describes the highly condensed and transcriptionally silent chromatin of the genome (Grewal and Jia, 2007). Rich in repetitive and non-coding sequences, and low in gene density, it has a characteristic chromatin organisation, many structural details of which remain unknown (Dillon, 2004). The DNA and histones of heterochromatin carry archetypal epigenetic modifications that are heritable through cell division. In addition to CpG DNA methylation, the constitutive heterochromatin environment is determined by histone modifications, such as trimethylation of histones H3 and H4 [histone H3 trimethyl Lys9 (H3K9me3), histone H4 trimethyl Lys20 (H4K20me3) and histone H3 trimethyl Lys64 (H3K64me3)] (Kourmouli et al., 2004; Schotta et al., 2004; Daujat et al., 2009). In mouse and *Drosophila*, a causal link between the first two marks led to the model that H4K20me3 is dependent on the recruitment of the methyltransferase suppressor of variegation 4-20 (Suv4-20) by chromobox homolog 5 (CBX5, also known as and hereafter referred to as HP1α, heterochromatin protein 1) bound to H3K9me3 through its chromodomains (Peters et al., 2002; Kourmouli et al., 2004; Schotta et al., 2004; Bongiorni et al., 2007).

Constitutive heterochromatin is mainly found at chromosome centromeres but also at telomeres, where it ensures the correct segregation and integrity of chromosomes (Fanti and Pimpinelli, 2008; Gartenberg, 2009). In addition, its chromatin environment causes the repression of genes within heterochromatin and in its vicinity. This includes genes at euchromatic loci that have been observed to relocate near heterochromatin in correlation with gene silencing (Dillon, 2004; Fedorova and Zink, 2008). Conversely, H4K20me3, together with H3K9me3 and HP1, were found to control imprinted gene expression by localising to silenced imprinted gene promoters and a non-expressed pseudogene (Delaval et al., 2007; Regha et al., 2007; Pannetier et al., 2008).

It is thought that the specification and maintenance of gene expression profiles in cell lineages during development involves an epigenetic control over gene regulation (Meehan et al., 2005). This was proposed to act through the limited availability for transcription of constitutive and facultative heterochromatin. These chromatin states are passed on to daughter cells, thus ensuring maintenance of tissue-specific expression patterns of genes (Fedorova and Zink, 2008). H4K20 methylation is essential for normal development, as implied by the finding that deletion of the Suv genes in mice, *Suv420h1* and *Suv420h2* (hereafter referred to as Suv4-20h for both) causes perinatal death (Schotta et al., 2008). Moreover, loss of H4K20me3 was reported in progressive cancers of both humans and animals (Fraga et al., 2005; Pogribny et al., 2006).

Previous reports have shown that the nuclear organisation of heterochromatin in pronuclear stage embryos is remodelled compared with its structure in mature somatic cells (Martin et al., 2006; Probst et al., 2007). Our detailed observations of chromatin during preimplantation mouse development provide further evidence of dynamic changes in heterochromatin and led to our discovery that the somatic pattern of heterochromatin is not established until late in development. Furthermore, comparisons between embryonic stem (ES) cells and the cells in the early embryo from which they are derived reveal important epigenetic differences, suggesting that ES cells rapidly acquire a more-mature chromatin profile during derivation. These results have many implications, which lead us to reassess and discuss the role of heterochromatin in differentiation and development.

Results

Epigenetic signature of mouse somatic heterochromatin and its remodelling after fertilisation

Mouse somatic cells, such as fibroblasts, stained with DAPI for DNA show a characteristic pattern of 10–20 bright dots in the

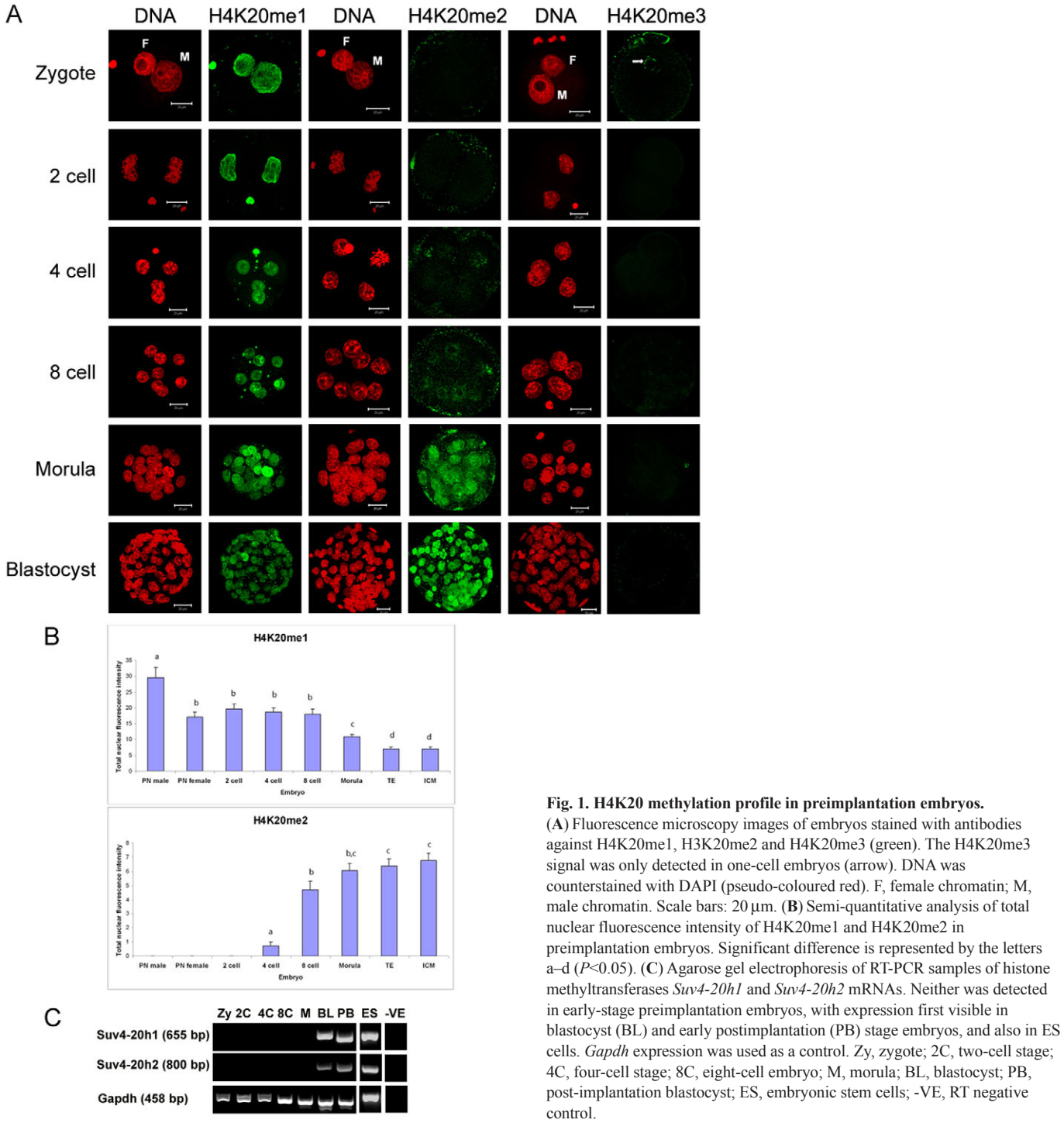

Fig. 1. H4K20 methylation profile in preimplantation embryos. (**A**) Fluorescence microscopy images of embryos stained with antibodies against H4K20me1, H3K20me2 and H4K20me3 (green). The H4K20me3 signal was only detected in one-cell embryos (arrow). DNA was counterstained with DAPI (pseudo-coloured red). F, female chromatin; M, male chromatin. Scale bars: 20 µm. (**B**) Semi-quantitative analysis of total nuclear fluorescence intensity of H4K20me1 and H4K20me2 in preimplantation embryos. Significant difference is represented by the letters a–d (P<0.05). (**C**) Agarose gel electrophoresis of RT-PCR samples of histone methyltransferases *Suv4-20h1* and *Suv4-20h2* mRNAs. Neither was detected in early-stage preimplantation embryos, with expression first visible in blastocyst (BL) and early postimplantation (PB) stage embryos, and also in ES cells. *Gapdh* expression was used as a control. Zy, zygote; 2C, two-cell stage; 4C, four-cell stage; 8C, eight-cell embryo; M, morula; BL, blastocyst; PB, post-implantation blastocyst; ES, embryonic stem cells; -VE, RT negative control.

nucleus that indicate areas of higher DNA density (supplementary material Fig. S1A). These regions of condensed chromatin correspond mainly to pericentromeric heterochromatin, which – in the acrocentric chromosomes of the mouse – is organised into chromocentres that join several chromosomes (Martens et al., 2005). These dots also show clearly when staining for DNA methylation, histone H3K9me3 and H4K20me3 methylation and HP1α (supplementary material Fig. S1A), confirming other reports (Peters et al., 2002; Kourmouli et al., 2004; Schotta et al., 2004) and consistent with the canonical epigenetic profile of constitutive heterochromatin (Martens et al., 2005). Uniquely in the mouse, the pericentromeric chromatin organisation allows direct microscopic observation of the most-abundant constitutive heterochromatin compartment in the nucleus. We have taken advantage of this to follow the formation of heterochromatin through development in terms of chromocentre appearance and epigenetic markers as detected with antibodies. These antibodies have been demonstrated to stain chromocentre heterochromatin in somatic cells in the literature (Peters et al., 2002; Schotta et al., 2004; Martens et al., 2005) as well as in our hands (supplementary material Fig. S1A, antibody panels).

Fertilisation is accompanied by decondensation of protamine-packaged sperm chromatin and metaphase-II-arrested oocyte chromosomes in the zygote (van der Heijden et al., 2005). Following pronuclear fusion and the first cell division, nuclear chromatin gradually takes on a more punctate pattern from four-cell stage onwards (Fig. 1A, all panels in DNA columns). Heterochromatic dots that resemble those of somatic cell nuclei become more evident towards the blastocyst stage (Fig. 1A, morula and blastocyst panels in DNA columns). These observations, consistent with other reports (Martin et al., 2006; Probst et al., 2007), are suggestive of important structural remodelling of the initially condensed pronuclear chromatin prior to the reestablishment of somatic heterochromatin, with the transition taking place over several embryo cleavage stages. We investigated whether this scenario is supported at the level of the molecular epigenetic marks of the histones and the DNA.

Distinct patterns of H4K20me1, H4K20me2 and H4K20me3 in preimplantation development

Our initial observations showed that some epigenetic markers present in somatic heterochromatin, such as H3K9me3 and CBX1 (also known as, and hereafter referred to, as HP1β), are detectable throughout preimplantation development together with changing levels of DNA methylation (Fig. 2, indicated rows, panels from zygote to blastocyst), supporting previous reports (Martin et al., 2006; Probst et al., 2007). We then focused on H4K20 methylation, as its trimethylated state is a constitutive heterochromatin marker. Differences in both the distribution and levels of mono-, di- and trimethylation of H4K20 were detected in cell nuclei during preimplantation development of mouse embryos. Only H4K20me1 was found in all preimplantation stages (Fig. 1A, zygote to blastocyst panels in H4K20me1 column). Semi-quantitative analysis of H4K20me1 fluorescence intensity showed that, in zygotes, H4K20me1 was preferentially enriched ($P<0.05$) in male chromatin compared with female chromatin. The signal was most intense from zygote to eight-cell stages and then became significantly reduced from morula to blastocyst stage (Fig. 1B). H4K20me2 was not found in zygotes or two-cell embryos, but was weakly visible at the four-cell stage and clearly detectable at morula stage (Fig. 1A, four-cell and morula panels in H4K20me2 column); there was no significant increase ($P>0.05$) in total nuclear intensity from morula to blastocyst (Fig. 1B). Moreover, there was no statistically significant

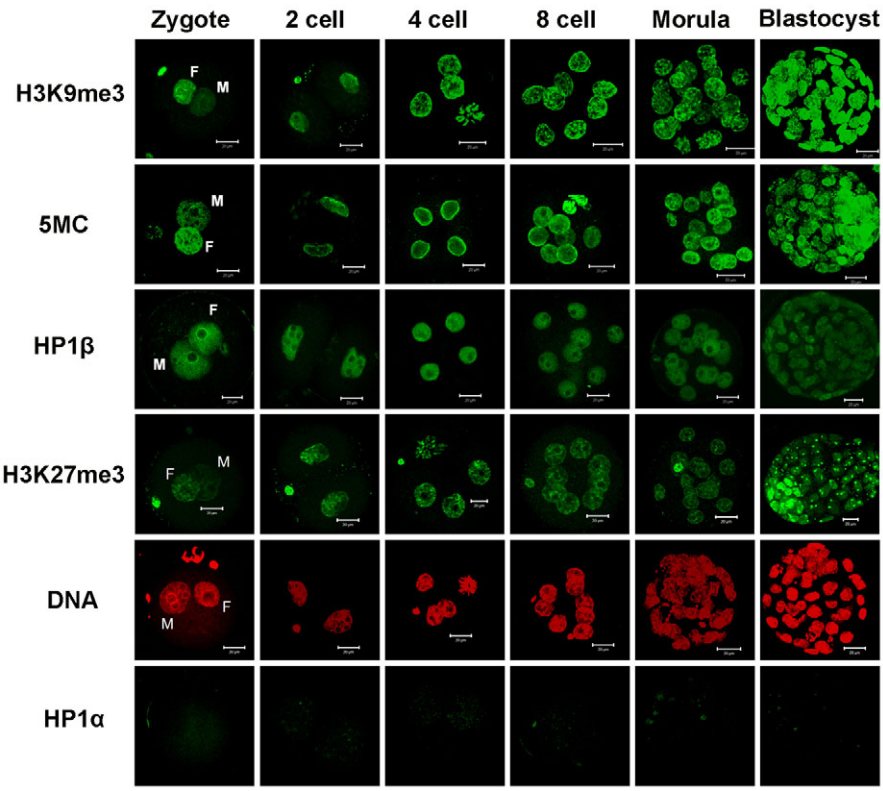

Fig. 2. Heterochromatin markers in preimplantation embryos. Immunofluorescence images of preimplantation embryos showing the heterochromatin markers (green) H3K9me3, 5-methyl cytosine (5MC), HP1β and H3K27me3, but not HP1α throughout preimplantation development. The last two rows depict absent or background HP1α signal relative to DNA (red) counterstained by DAPI. F, female chromatin; M, male chromatin. Scale bars: 20 μm.

difference between trophectoderm (TE) and inner cell mass (ICM) for either H4K20me1 or H4K20me2 (Fig. 1B).

H4K20me3 was found only in the female chromatin of the zygote, where it was localised specifically at the perinucleolar rings (Fig. 1A, zygote panel in H4K20me3 column), in which pericentric heterochromatin resides at this stage (Probst et al., 2007). In our studies, H4K20me3 was completely undetectable by the two-cell stage (Fig. 1A, H4K20me3 column). The apparent demethylation of H4K20me3 between the pronuclear and two-cell stages is consistent with a previous observation that the level of H4K20me3 was hardly detectable in two-cell embryos (Kourmouli et al., 2004). In notable contrast to its strong presence in embryonic fibroblasts using the same antibody (supplementary material Fig. S1A, H4K20me3 antibody panel), we show that H4K20me3 signal remains undetectable for the whole of preimplantation development (Fig. 1A, H4K20me3 column).

Immature heterochromatin in the preimplantation embryo

Closer inspection of our immunofluorescence data showed that heterochromatic marks associated with nuclear DNA foci in somatic cells (supplementary material Fig. S1) had distinct distributions during preimplantation stages (Fig. 2, compare rows H3K9me3, 5MC, HP1β, HP1α and DNA). H3K9me3 and meCpG converged with the DNA punctate pattern forming at later stages (Fig. 2). Unlike in somatic cells, in which HP1β is predominantly found in heterochromatin (Gilbert et al., 2003; Ayoub et al., 2008), HP1β in preimplantation embryos was distributed throughout the nuclei of interphase cells (Fig. 2, all panels in HP1β row), confirming previous reports (Martin et al., 2006; Probst et al., 2007). Surprisingly, we found that HP1α, which is commonly present in constitutive heterochromatin of somatic cells (supplementary material Fig. S1A), is undetectable in all developmental stages before implantation (Fig. 2, no signal in all panels for HP1α, compare with respective panels for DNA). This observation is comparable to those made by van der Heijden et al. but not to those made by Houlard et al. (van der Heijden et al., 2005; Houlard et al., 2006). Taken together, our immunocytochemistry studies (Figs 1, 2) indicate that two epigenetic markers for constitutive heterochromatin in somatic cells, H4K20me3 and HP1α, are absent from preimplantation embryos, whereas DNA methylation, H3K9me3 and HP1β are detectable throughout preimplantation development.

Using pooled embryo samples, we conducted an RT-PCR analysis of the mRNA levels for the *Suv4-20h* histone methylases responsible for the H4K20me3 modification. We found that they were undetectable in early preimplantation embryos but present in periimplantation blastocyts (Fig. 1C). The lack of H4K20me3, HP1α and Suv4-20h indicates that heterochromatin in preimplantation embryos is significantly different from that in somatic cells, leading us to suggest that it is in an immature state.

Heterochromatin matures postimplantation during gestation

The next question was, at which stage of embryo development mature heterochromatin is established. As the earliest implantation stages of in vivo development are difficult to study, we initially used in vitro embryo attachment as a model for early stages of implantation (day 5.5–6.5 of gestation) (Nishi et al., 1995). After whole blastocysts were placed into medium, trophectoderm began to differentiate to trophoblast followed by attachment to the plate by 24–48 hours. Intriguingly, H4K20me3 and HP1α, which were not found in preimplantation blastocysts (Fig. 3, in vitro preimplantation, H4K20me3) (supplementary material Fig. S2, HP1α), were detected after this in vitro 'implantation'. H4K20me3 was first detected only in cell nuclei of mural TE, not in polar TE or in ICM positive for octamer 4 (Oct4) (Fig. 3, in vitro postimplantation, compare H4K20me3 with Oct4), whereas HP1α was hardly detectable at 24 hours but visible at 48 hours (supplementary material Fig. S2). By 4 days, the ICM outgrowth and giant trophectoderm had enlarged, and both H4K20me3 and HP1α staining were strong in giant trophoblast as well as ICM-derived cell colonies (supplementary material Fig. S7, HP1α). Whereas giant TE nuclei showed a nuclear punctate pattern typical for heterochromatin, the signal in ICM colonies was more diffuse (supplementary material Fig. S7, compare cells inside and outside the colony).

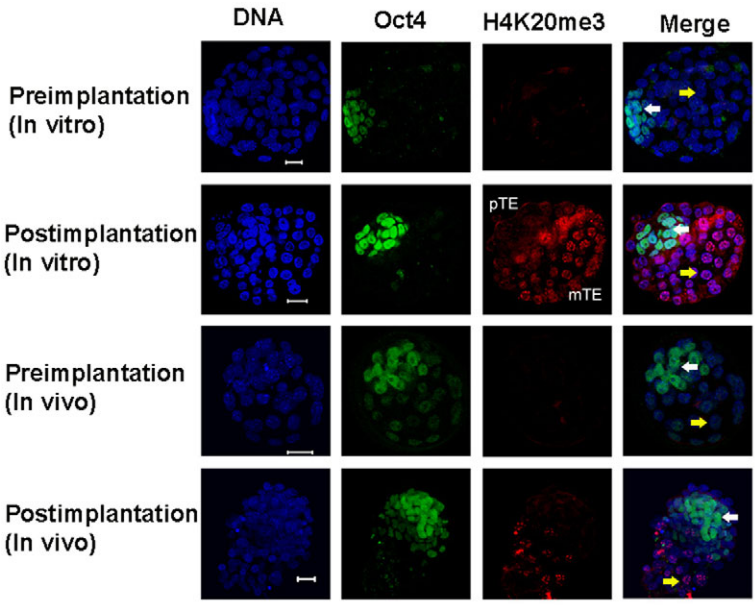

Fig. 3. Remethylation of H4K20me3 postimplantation. Pre- and postimplantation blastocysts from in vitro culture or ex vivo collection were double immunostained for Oct4 (green) and H4K20me3 (red); DNA was counterstained with DAPI (blue). ICM cells stained positive for Oct4. Preimplantation embryos were negative for H4K20me3. Postimplantation embryos stained positive for H4K20me3 in the mural trophectoderm (mTE) but not the polar trophectoderm (pTE). White arrows points to ICM cells, yellow arrows indicate trophectoderm cells. Scale bars: 20 μm.

In agreement with these in vitro observations, mouse embryos retrieved around the time of in vivo implantation showed no detectable H4K20me3 at E3.5 (Fig. 3, in vivo preimplantation) but stained positive for this marker at E4.5, when it was only found in mural TE but not in polar TE or in ICM (Fig. 3, in vivo postimplantation, H4K20me3 and Oct4). Next, we investigated the first occurrence of H4K20me3 and HP1α in postimplantation embryo development. In whole-mount embryos dissected ex vivo at stages E5.5–E6.5 (early postimplantation), H4K20me3 was undetectable in interphase nuclei, as was HP1α (E5.5 shown in Fig. 4, H4K20me3 and HP1α). To test for another heterochromatin marker, and also as a control for our whole-mount immunodetection protocol, postimplantation embryos were stained with an antibody against H3K9me3. The corresponding panel in Fig. 4 shows H3K9me3 in both epiblast (derived from ICM) and extraembryonic ectoderm (derived from polar TE). This is consistent with its presence throughout preimplantation development (Fig. 2) and confirms that our protocol allows antibody to penetrate into both these tissues. Furthermore, sections of implantation sites in utero show H4K20me3 nuclear foci in the maternal and trophectoderm-derived foetal placenta (supplementary material Fig. S3).

Analysis of cryosections of E7.5 embryos, and E11.5, E14.5 and E17.5 foetuses showed that despite the formation of the germ layers and increased structural complexity (Fig. 5, diagram) H4K20me3 and HP1α were not detected at E7.5, whereas H3K9me3 immunostaining was positive (Fig. 5, E7.5). In E11.5 foetuses, post mid-gestation (diagram), HP1α was detected as a weak and diffuse nuclear signal compared with that for H3K9me3, but H4K20me3 remains below detection levels (Fig. 5, E11.5). However, both HP1α and H4K20me3 were clearly present in E14.5 foetuses (Fig. 6A, E14.5) in derivatives of all three germ layers. At this stage, in brain tissue some cell nuclei contained weak dots whereas other cells stained in a diffuse pattern. At stage E17.5, both marks had adopted a strong heterochromatic pattern colocalising with DNA dense foci (Fig. 6A, E17.5 brain panels). A similar case was found in liver tissue, where the H4K20me3/HP1α heterochromatin foci seemed less abundant at E17.5 while diffuse signals remained in some nuclei (Fig. 6A, E17.5 liver panels). This was even more pronounced in bone marrow tissue, where few heterochromatic foci were apparent at E17.5 (Fig. 6A, E17.5 bone panels; supplementary material Fig. S4, Gata4-positive control). Overall, based on the presence of H4K20me3 and HP1α, our results suggest that these heterochromatin markers are acquired slowly during foetal development, first as a diffuse nuclear signal which subsequently concentrates into heterochromatic foci. Although a previous study (Biron et al., 2004) reported the presence of H4K20me3 in E8.5 and E11.5 localised brain structures, their results did not identify a clear nuclear pattern of this marker at the earlier stage. Nevertheless, foetal cell types may vary in heterochromatin maturation rates, as bone marrow tissue remained relatively unchanged between E14.5 and E17.5 embryos in contrast to brain tissue. Furthermore, co-staining for nestin within E17.5 brain tissue to highlight neuronal precursor cells showed lower levels of H4K20me3 in a presumptive proliferative zone containing nestin filaments compared with the adjacent region (Fig. 6B). Together, these findings suggest that a mature heterochromatin profile is associated with more-differentiated cell lineages.

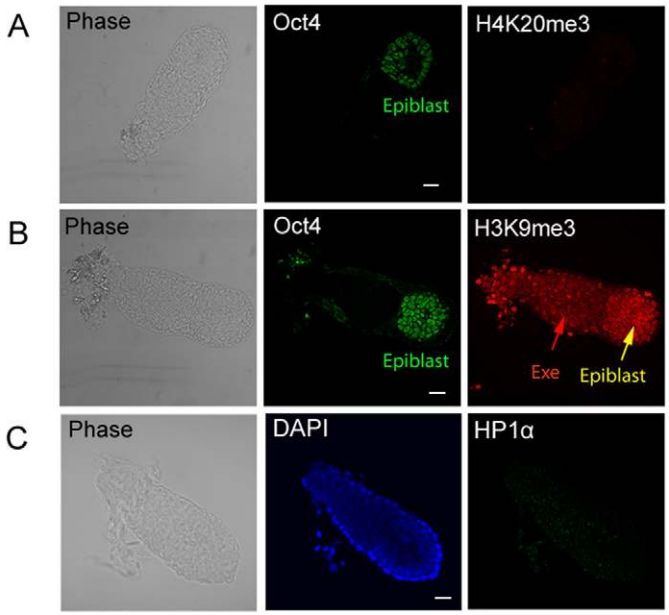

Fig. 4. H3K9me3, but not H4K20me3 and HP1α, was found in early postimplantation embryos. Whole-mount immunofluorescence and phase-contrast images of in vivo postimplantation embryos (E5.5). (**A**) Double immunostaining of embryos show epiblast cells that stained positive for Oct4 (green) but the embryo was negative for H4K20me3 (red). (**B**) Double immunostaining of embryos show the whole embryo stained positive for H3K9me3 (red), whereas only the epiblast stained positive for Oct4 (green). Exe, extraembryonic ectoderm. (**C**) Immunostaining of embryos counterstained with DAPI (blue) shows embryos were negative for HP1α (some residual background signal is visible). Scale bars: 20 μm.

In vitro culture induces maturation of constitutive heterochromatin

Whereas our results and several earlier reports (Kourmouli et al., 2005; Martens et al., 2005; Benetti et al., 2007; Dialynas et al., 2007) identified H4K20me3 and HP1α in ES cells (supplementary material Fig. S1B), we had not found these marks in ICM or epiblast (Figs 3, 4). We, therefore, hypothesised that H4K20me3 and HP1α are induced in ES cell nuclei during derivation. To test this, ES-like cells were isolated from blastocysts using standard ES-cell derivation procedures (Nagy et al., 2006a), and compared with ICM and epiblast. The cells that were obtained exhibited ES cell morphology, were Oct4- and NANOG-positive (Fig. 7A), and were able to form embryoid bodies and beating cardiomyocytes after differentiation (supplementary material Fig. S5). Nevertheless, in our experiments, these ES-like cell nuclei had already expressed H4K20me3 and HP1α in the first three passages of cells (Fig. 7A) to levels comparable with those of an established ES cell line (E14tg2a, supplementary material Fig. S1B) – in stark contrast to the absence of these markers in ICM (Fig. 3, Oct4-positive cells) or epiblast (Fig. 4).

These results suggest that emergence of H4K20me3 and HP1α in ES cell nuclei (and embryos) can be induced after in vitro culture, possibly by factors in the culture medium. To test this, we first cultured preimplantation blastocysts in ES cell medium with or without leukemia inhibiting factor (LIF), a factor required in the ES cell derivation protocol (Nagy et al., 2006a). LIF, indeed, influenced the kinetics of appearance of the H4K20me3 marker, occurring at ~24 hours in medium without LIF and ~48 hours in medium containing LIF. Immunofluorescence results, however, did not show any difference in the distribution pattern of H4K20me3 when comparing LIF-containing and LIF-free medium

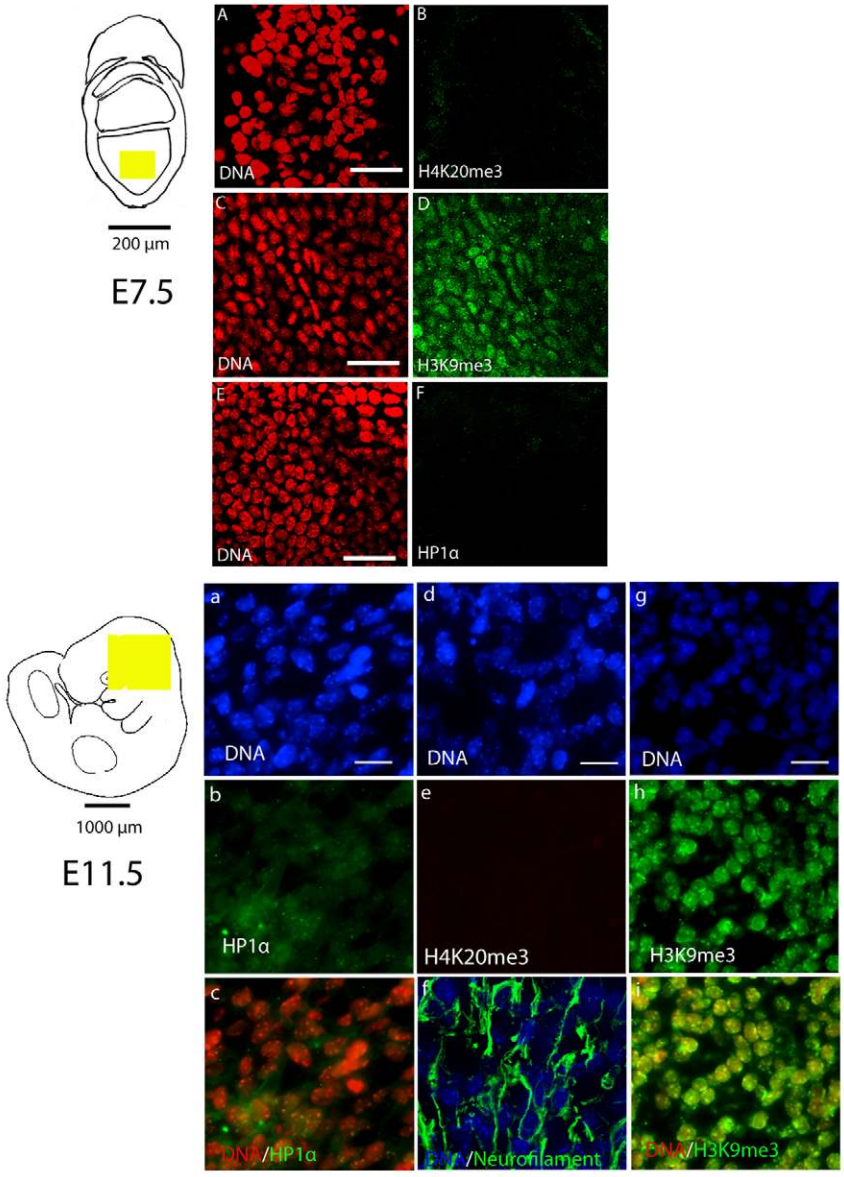

Fig. 5. Heterochromatin markers H4K20me3 and HP1α in E7.5 and E11.5 embryos. E7.5 embryos (whole mount) and E11.5 embryos (cryosections) were immunostained for the heterochromatin markers H3K9me3, H4K20me3 and HP1α (green fluorescence). (**A-F**) E7.5 embryos were negative for H4K20me3 (B) and HP1α (F) but stained positive for H3K9me3 (D). Nuclei are visualised by DAPI counterstaining (A,C,E, pseudo-coloured red). The images correspond to the area highlighted in yellow in the diagram, containing ectoderm and mesoderm. (**a-i**) In E11.5 foetal tissue, HP1α (b) and H3K9me3 (h) were detected, but not H4K20me3 (e). HP1α at E11.5 was mainly found in a diffuse nuclear pattern that does not overlap with regions of dense DNA (c, merge), whereas theH3K9me3 signal overlapped substantially with that of DNA (i, merge). The images correspond to the area highlighted in yellow in the diagram containing brain neurons, as confirmed by staining with anti-neurofilament antibody (f, green fluorescence). DNA counterstained with DAPI is shown in blue (a,d,g,f) or pseudo-coloured red (c,i). Scale bars in microimages: 20 μm.

(supplementary material Fig. S6). We also tested whether omission of non essential amino acids and β-mercaptoethanol, which are usually included in ES medium, had any impact, and found that this did not alter the occurrence of H4K20me3 and HP1α (supplementary material Fig. S6). Moreover, we tested trophectodermal stem (TS) cell medium based on RPMI-1640 plus FGF4 and heparin, which is commonly used to isolate TS cells (Quinn et al., 2006). Compared with ES cell medium, culture of preimplantation embryos in TS cell medium resulted in smaller colonies that resembled cells derived from polar trophectoderm and almost all of the cells stained positive for H4K20me3 and HP1α (supplementary material Fig. S7).

The partial effect of LIF, a cytokine that in combination with either serum or bone morphogenic protein (BMP) allows the derivation and maintenance of mouse ES cells, prompted us to further investigate ES derivation conditions that may produce epigenetic differences relative to ICM. We first compared ES cells cultured in medium supplemented with either foetal bovine serum (FBS) or serum replacement (SR). No differences in the level or nuclear pattern of H4K20me3 and HP1α were noticeable in immunofluorescence (Fig. 7B) or western blot (Fig. 7C) of ES cells cultured with or without serum. By contrast, there were substantial changes in other modifications and heterochromatin proteins: in the absence of serum, H3K9me3 levels were increased whereas levels of H4K20me1 and HP1β were decreased (Fig. 7C). We then tested a two-inhibitor (2i) medium that was reported to keep ES cells in a ground state by shielding pluripotent cells from differentiation-inducing stimuli (Ying et al., 2008). However, this 2i ES cell medium, which contains the mitogen-activated protein kinase kinase (MEK) inhibitor PD0325901 and the glycogen synthase kinase 3β (GSK3β) inhibitor CHIR99021, as well as BMP4, did not affect the presence of H4K20me3 and HP1α in ES cells (Fig. 7C). Finally, we cultured ES cells under low-oxygen atmosphere (5% O_2) because in utero development is believed to be naturally hypoxic. Culturing in low oxygen conditions dramatically reduced the amount of HP1α to levels undetectable by immunofluorescence. Whereas H4K20me3 was still present in most ES cells, the weak speckled pattern within the nucleus became

more diffuse (Fig. 7C), possibly because HP1α did not recruit H4K20me3 to the pericentric heterochromatin.

Taken together, we found that LIF can delay the onset of H4K20me3 and HP1α, and culturing in conditions of low oxygen can reduce the level of HP1α. Both LIF and low-oxygen conditions are found in oviduct and uterus. Nevertheless, adding LIF to medium and incubating cells under low oxygen still could not prevent trimethylation of H4K20me3. This might be owing to further differences between preimplantation and ES cell derivation, because in vivo development of ICM and epiblast is influenced by cell–cell interactions from the neighbouring primary endoderm, trophectoderm and extraembryonic ectoderm.

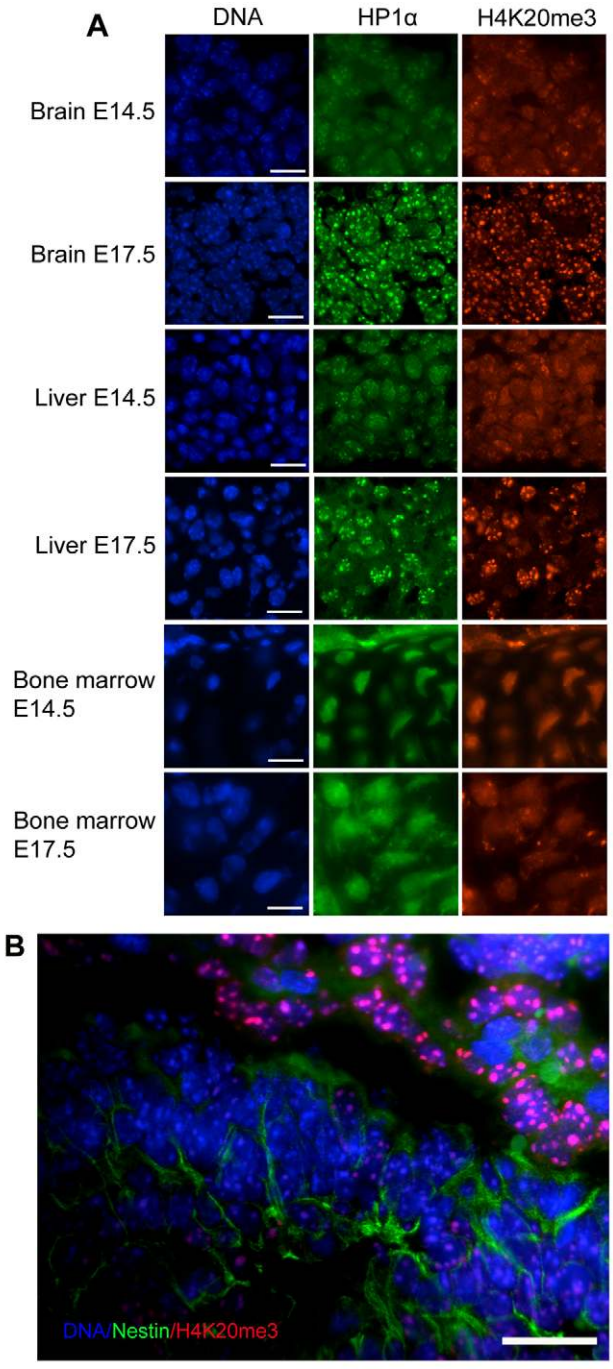

Fig. 6. H4K20me3-positive cells increase during late gestation. (**A**) Immunofluorescence images of cryosectioned foetal tissue (brain, liver and bone marrow) from E14.5 and E17.5 late-gestation stages stained for H4K20me3 (red) and HP1α (green). DNA was counterstained with DAPI (blue). The number of nuclei with strong punctate signal increases between E14.5 and E17.5 in brain and liver but not bone marrow. (**B**) Forebrain was double stained for nestin (green) and H4K20me3 (red). Nestin-positive cells appear to stain less for H4K20me3 compared with nestin-negative cells. Scale bars: 20 μm.

Dynamic patterns of H4K20me3 and HP1α in ES cells

Intriguingly, we found that, in ES cells, H4K20me3 and HP1α presented two different nuclear patterns: diffuse distribution and showing as punctate foci. The correlation between HP1α and H4K20me3 after double immunofluorescence labelling is shown in Fig. 8. Cells can be classified into three types: type I has diffuse HP1α distribution and shows very weak H4K20me3 immunofluorescence signals (Fig. 8, left column). In type II HP1α distribution is punctate, whereas that of H4K20me3 is diffuse (Fig. 8, middle). In type III both HP1α and H4K20me3 distributions are punctate (Fig. 8, right).

Randomly captured fluorescent images of 1000 cell nuclei were each allocated to one of these three categories. The percentages for type I, II and III were 10%, 54% and 36%, respectively. Importantly, we did not observe cells with a punctate H4K20me3 distribution and a diffuse HP1α distribution pattern. Notably, after ES cell differentiation only type III cells were found. Our results suggest that, although ES cell nuclei acquire all heterochromatin markers during derivation, the heterochromatin is still highly dynamic.

H4K20me3 and cell differentiation

Our finding that H4K20me3 can first be detected postimplantation prompted us to investigate whether it is associated with cell lineage specification. Using ES cell differentiation and in vitro implantation as models for cell differentiation, we analysed the correlation between the appearance of H4K20me3 at pericentric heterochromatin foci and the levels of the pluripotency marker Oct4. This was to test the hypothesis that H4K20me3 increases in nuclei after the cells lose Oct4 during differentiation.

Microscopic analysis of, initially Oct4-positive, ES cell populations and outgrowths of in vitro embryo attachments was performed following 2 weeks of differentiation in culture. Fig. 9A shows that, at low levels of Oct4, the proportion of strongly H4K20me3-positive cells was 26% (60 cells out of 230) in differentiated ES cells and 64% (135 cells out of 210) in in-vitro implantation cells. Differentiation after in vitro implantation is likely to be more highly correlated with H4K20me3 than in the ES cell differentiation model; however, the difference may reflect the technical difficulty in obtaining cells at the same stage of differentiation in the two models. Importantly, 35% (95 cells out of 270) of differentiated ES cells and 31% (90 cells out of 290) of in vitro implanted cells had increased levels of H4K20me3, whereas Oct4 was still clearly detectable. These results imply that, during differentiation, H4K20me3 increased before there was a substantial reduction of Oct4.

Additionally, western blots were used to analyze global heterochromatin modification changes during ES cell differentiation into embryoid bodies. After induction of embryoid body formation (day 7), histone H3K9me3 trimethylation increased, but HP1β protein levels decreased, whereas H4K20me3 and HP1α did not change substantially overall (Fig. 9B).

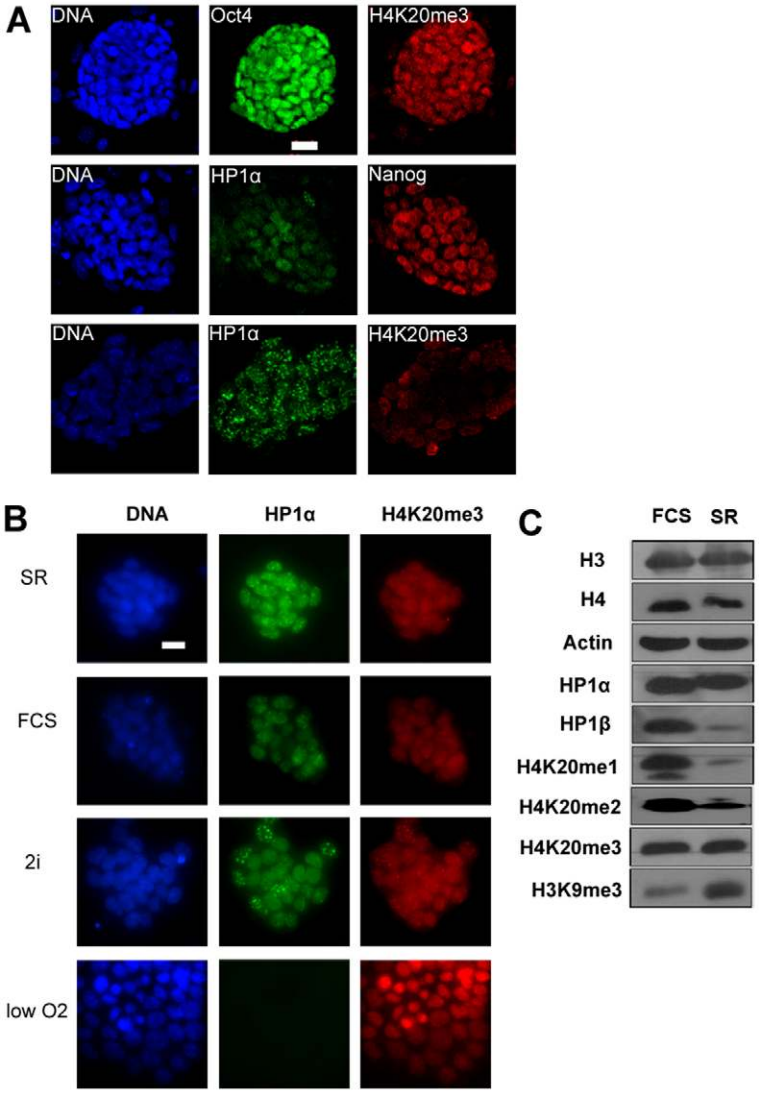

Fig. 7. H4K20me3 and HP1α are induced during ES cell derivation. (**A**) H4K20me3 (red) and HP1α (green) immunostaining was found in the first passage of ES-like cells that also stained positive for Oct4 (green) and NANOG (red). The images show double immunofluorescence and DAPI counterstaining (blue) of three early colonies. Scale bar: 20 µm. (**B**) Effect of culture conditions on H4K20me3 and HP1α in ES cells. Culture with foetal calf serum (FCS), serum replacement (SR) or the two inhibitors CHIR99021 and PD0325901 (2i) did not alter H4K20me3 and HP1α, but at conditions of low (5%) O_2 (low O2) HP1α was not detected and H4K20me3 showed a diffuse pattern. Scale bar: 20 µm. (**C**) Western blot analysis of chromatin modifications in ES cell cultures that had been derived in the presence or absence of FCS, show similar levels of H4K20me3 and HP1α compared to those of histones H3 and H4, and actin controls, whereas changed levels are observed for other markers. FCS, ES cells cultured in medium supplemented with ES-cell-qualified FCS; SR, ES cells cultured in medium supplemented with knockout serum replacement.

Finally, we used flow cytometry to measure the fluorescence intensity of individual ES cells in a population of $>10^4$ cells. We observed a weak correlation between higher levels of HP1α and H4K20me3 and lower levels Oct4 in two subpopulations within normal ES cell cultures that could be partially separated on the basis of granularity characteristics (Fig. 9C, green trace and red-filled peaks). Taken together, flow cytometry and microscopy results suggest that H4K20me3 and HP1α are preferentially enriched in cells that show lower Oct4 immunofluorescence, whereas western blots indicate unchanged levels within the Oct4-expressing ES cell population as a whole. Consistent with several reports showing that ES cells are a heterogeneous population with regards to the pluripotent markers NANOG (Chambers et al., 2007; Singh et al., 2007), Rex1 or Oct4 (Toyooka et al., 2008), or SSEA1 (Furusawa et al., 2006), these subpopulations might represent early differentiation transitions (Chambers et al., 2007; Singh et al., 2007; Toyooka et al., 2008) or harbour an early chromatin disposition for cell differentiation (Bernstein et al., 2006).

Discussion

Our study of the cell nuclear chromatin organisation in mouse embryos provides new insights into heterochromatin formation by revealing dynamic changes in heterochromatin patterns during preimplantation and postimplantation development that continue well into late gestational stages. In addition, we have identified marked epigenetic differences between ES cells and the blastocyst ICM cells from which these ES cells are derived. These results demonstrate that heterochromatin undergoes a maturation process, which is relevant to understanding how epigenetic modifications on histones and DNA help maintain and propagate heritable cell type characteristics during development as well as in tissue culture. This in turn may provide potential markers to assess the epigenetic profile of cells in normal differentiation and disease, including the effects of tissue culture on in-vitro-assisted reproduction and nuclear programming.

H4K20me3 and HP1α – late developmental heterochromatin markers

Our mouse developmental study reports the surprising finding that constitutive heterochromatin as currently defined is a mainly somatic state of heterochromatin forming after slow maturation during development. We demonstrate that two hallmarks of constitutive heterochromatin in somatic cells, H4K20me3 and HP1α, are absent during much of mouse development. These

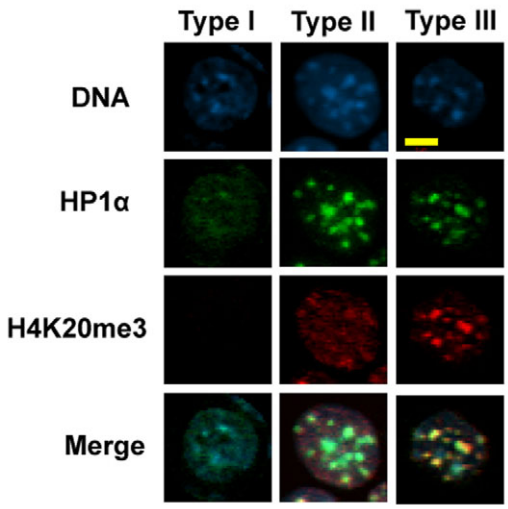

Fig. 8. H4K20me3 in ES cell cultures and in-vitro-attached embryo outgrowths. Three dynamic categories of ES cells (E14tg2A) were investigated on the basis of their staining pattern of H4K20me3 (red) and HP1α (green). Scale bar: 5 μm.

heterochromatin markers disappear from the maternal genome before fertilisation (Fig. 1A, Fig. 2), and do not reappear in most tissues until well after mid-gestation.

Heterochromatic silencing is proposed to have a role in maintaining cell-lineage-specific epigenetic patterns of gene expression (Dillon, 2004; Meehan et al., 2005; Grewal and Jia, 2007). This is primarily based on the capacity for propagation of this condensed chromatin structure through cell division. It is assumed that the heritability of the heterochromatin structure resides in the histone modifications in addition to DNA methylation. The widely varying onset of appearance of various heterochromatin marks relative to the cell lineage specification process may therefore indicate their potential involvement in this process. Whereas the link between H3K9me3 and gene repression is more straightforward than between H4K20me3 and gene silencing (Barski et al., 2007), H3K9me3 is already present in heterochromatin from the early cleavage stages of the undifferentiated embryo. H3K64me3 appears at the blastocyst stage and is not localised to genes (Daujat et al., 2009). This study shows that H4K20me3 does not mark the onset of differentiation in the tissues of the embryo. Instead, it marks cells in late foetal development when organs and tissues have been formed.

It is, nevertheless, plausible that the sequence of appearance of epigenetic chromatin markers contributes to the varying requirements of constitutive heterochromatin during cell lineage specification. An important exception to the late developmental appearance of the H4K20me3 mark occurs during the early differentiation of blastocyst cells into the extra-embryonic cells of the mural trophectoderm. In these cell nuclei, H4K20me3 becomes detectable after in vitro implantation as well as in utero development. This might be explained by the characteristics of the mural trophectoderm lineage, in which cell division slows after their proliferation from the polar trophectoderm, whereas DNA replication continues as the cells terminally differentiate into polyploid invasive giant trophoblast cells (Hemberger, 2007). If we consider that differentiation starts with the loss of pluripotency but continues through development during further lineage

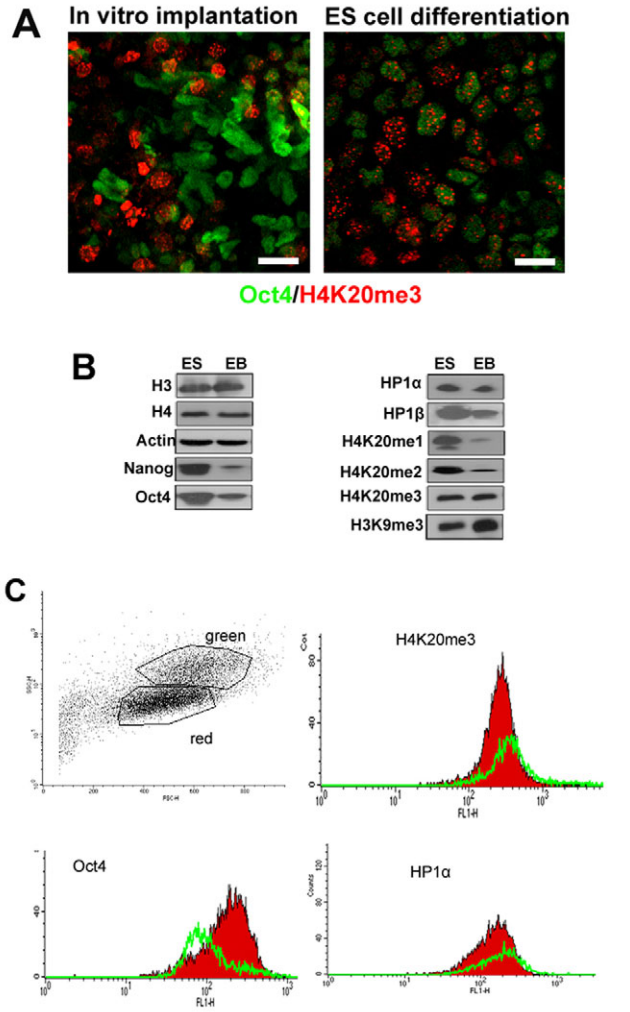

Fig. 9. Chromatin modification and cell differentiation. (**A**) Double immunofluorescence staining of cells that had been derived after 2-weeks-in vitro implantation and of differentiated ES cells for Oct4 (green) and H4K20me3 (red). More overlap between markers is visible after ES cell differentiation. Scale bars: 20 μm. (**B**) Western blot analysis of ES cells (ES) and embryoid bodies (EB) reveal differences in the global epigenetic profile when pluripotent cells (ES cells) are compared with early-differentiation cells (embryoid bodies); no differences are observed in the levels of H4K20me3 and HP1α. (**C**) Flow cytometry analysis of ES cells shows heterogeneous populations on the basis of the staining signals of H4K20me3 and HP1α, which appear to be enriched in cells that have lower Oct4 levels.

specification, the mural trophectoderm presence might be indicative of a link between H4K20me3 and terminal differentiation of cell lineages during development. A previous study in midgestation mouse embryos suggested that H4K20me3 is associated with neural and muscle cell differentiation (Biron et al., 2004). In further support of a link with late differentiation are the regional differences we observed in the appearance of histone H4K20me3 trimethylation and HP1α protein: nuclear staining patterns in bone marrow remained more diffuse than in liver tissue and differentiated neural tissue, respectively (Fig. 6A). Within brain tissue, nestin positive progenitor cells were seen to stain less brightly for H4K20me3 (Fig. 6B).

Our study shows that H4K20me3 levels increase in late development. This is consistent with previous reports: mass spectrometry has shown that liver and kidney cells from senescent animals contain more H4K20me3 than young animals (Sarg et al., 2002); two studies using human cell lines in which H4K20me3 was low have shown that H4K20me3 increased in late-passage cells or non-growing cells (Sarg et al., 2002; Shumaker et al., 2006). Furthermore, global and specific gene expression analysis in human neural development has shown that H4K20me3 is upregulated in adult mature cerebellum compared with immature cerebellum from foetuses and infants and is not related to gene transcription (Stadler et al., 2005). Together these results support that H4K20me3 could be correlated to tissue maturation or ageing.

Chromatin differences between ICM and ES cells

We report the reproducible presence of H4K20me3 and HP1α in newly established ES cells, which is in contrast to embryonic development where H4K20me3 and HP1α are late heterochromatic markers. This suggests that by the time ES cells are established they have acquired a more-mature, somatic form of heterochromatin compared with the ICM cells from which they originate. This conclusion is at odds with the idea that ES cells are equivalent to ICM cells, at least in terms of their chromatin organisation, but is supported by previous studies showing that the chromatin marker H2A.Z is not detected in the ICM but is present after in vitro implantation (Rangasamy et al., 2003) and also in ES cells (Creyghton et al., 2008). In addition, several studies have reported differences in transcription profiles of ES cells and ICM (Horie et al., 1991; Toyooka et al., 2003; Clark et al., 2004; Reijo Pera et al., 2009). Recently, Dahl et al. have reported that levels of H3K4me3 and H4K27me3 on gene promoters in ES cells differs from ICM (Dahl et al., 2010).

The acquisition of a somatic heterochromatin profile in ES cells can be explained in part by the cell culture conditions. Supplementation of LIF, normally produced in the embryo by TE and necessary for ES derivation, delayed trimethylation of H4K20me3. By testing other intra-embryonic cell–cell signals and investigating conditions that are not met in cultured cells, we found that reinstating the low oxygen levels in which embryonic development normally takes place had the most-pronounced effect, reducing HP1α to undetectable levels. A probable mechanism for this has been suggested by reports that hypoxia activates the JAK2/STAT3 signalling pathway (Wang et al., 2010). Although LIF is known to activate STAT3 through this pathway, recent findings have shown that JAK signalling can also directly control heterochromatin stability (Li, 2008; Griffiths et al., 2011). In particular, phosphorylation of histone H3Y41 by JAK2 reduces HP1α binding to H3 (Dawson et al., 2009), possibly explaining our chromatin effects. In addition, heterochromatin maturation could be envisaged as an accumulative process. Considering that ICM cells normally only exist during a short time window in the embryo before differentiation sets in, forcing the cells to perpetuate a normally transitory state might somehow affect the heterochromatin such that it adopts the configuration of a stable ‘not differentiating’ cell lineage. A recent expression analysis of key epigenetic regulators suggested that ES cells have a globally more repressive epigenetic status compared with the ICM. This was linked to the ICM cells undergoing rapid developmental changes, requiring greater epigenetic flexibility (Tang et al., 2010).

ES cells, nonetheless, remain self-renewing in terms of their pluripotency despite having acquired heterochromatin markers H4K20me3 and HP1α. ES cells also tolerate the loss of heterochromatin markers H3K9me3 (Lehnertz et al., 2003) or H4K20me3 (Benetti et al., 2007). These results imply that the ES cell heterochromatin profile does not affect their pluripotent state, although it may be associated with their capacity for differentiation or maintaining differentiated states.

Mechanism of heterochromatin maturation

It has been shown in somatic cells that H4K20me3 marks heterochromatin dependent on the presence of HP1 and Suv4-20h enzymes (Kourmouli et al., 2005; Schotta et al., 2004). There is supporting evidence from the present developmental study. First, H4K20me3, HP1α and Suv4-20h are all deficient in preimplantation embryos, whereas in mural trophectoderm as well as foetal development, the late appearance of H4K20me3 seems connected to the presence of HP1α. Second, ES cells show a dynamic correlation between HP1α and H4K20me3 levels, where the pattern of H4K20me3 seems to depend on HP1α (Fig. 8). Comparison of the nuclear distributions of the two markers showed that H4K20me3 does not display condensed punctate staining unless it colocalises with HP1α. Other cells, presumed to be at a less-organised nuclear stage, showed a diffuse nuclear distribution for both markers. Interestingly, diffuse nuclear H4K20me3 patterns also occurred when HP1α was present as a punctate pattern.

On first reflection, our data are consistent with the model proposing that HP1 is necessary to establish H4K20me3 in heterochromatin (Kourmouli et al., 2004; Schotta et al., 2004); however, the lack of colocalisation in some cases suggests recruitment of chromatin that is already marked with H4K20me3 (but where levels of HP1 are low or not existent) into HP1-containing chromocenters or foci. How the diffuse H4K20me3 distribution can be reconciled with the model of the Suv4-20 methylating enzyme by HP1α at nucleosomal level (Kourmouli et al., 2004; Schotta et al., 2004) remains to be determined. We also noticed that, in mural trophectoderm, H4K20me3 becomes detectable shortly before HP1α. Nevertheless, in development, this connection would control the timing of these two hallmarks of constitutive heterochromatin, and their joint late presence in development reinforces the observation of the late formation of mature condensed chromatin during development.

The loss of H4K20me3 early in the preimplantation embryo might result from a lack of HP1α and Suv4-20h enzymes, as Suv4-20h and HP1α transcripts only become detectable after implantation or ES cell derivation (Fig. 1C; HP1α not shown). Although active histone demethylation might be another potential factor, no H4K20me3 demethylase has as yet been reported. Whereas histone demethylase JMJD2A has a domain that is specific for H4K20me3, it has shown no functional activity in removing H4K20me3 (Lee et al., 2008).

H4K20me3 and cell differentiation

A number of different studies have suggested that ES cell chromatin is less compact and more transcription-permissive than that of differentiated cells (Table 1). First, ES cells have only a small number of heterochromatin foci, which increases after cell differentiation (Kobayakawa et al., 2007). Second, fluorescent recovery after photobleaching (FRAP) results have suggested that most chromatin proteins in ES cell are hyperdynamic and bound more loosely to chromatin than in differentiated cells (Meshorer et al., 2006). Third, global transcription in ES cells is hyperactive and is substantially reduced after differentiation (Efroni et al., 2008).

Table 1. The presence and pattern of heterochromatin markers

Location	H4K20me3	HP1α	HP1β	Open chromatin
Preimplantation to postimplantation (E5.5–E7.5)	Absent or very weak	Absent or very weak	Diffuse	+++
Foetus	Foci	Foci	Foci	+
ES cell	Foci or diffuse staining pattern	Foci or diffuse staining pattern	Foci	++
Differentiated cell	Foci	Foci	Foci	+

+, ++ and +++ indicate low, medium and high levels of open chromatin, respectively.

Fourth, repetitive sequences including those in pericentric heterochromatin, are transcriptionally active in ES cells, but in differentiated cells repeated regions are silenced by increasing repressive epigenetic markers (Martens et al., 2005; Efroni et al., 2008). The differences in presence and pattern of H4K20me3, HP1α and HP1β described in our study might account for these differences in chromatin structure. However, our ES cell differentiation experiments show that, despite a weak inverse correlation at cell level, H4K20me3 can coexist with Oct4 and is independent from the differentiation process.

H4K20me3 – a heterochromatin maintenance marker?

The presence of H4K20me3 in two chromatin states at opposite ends of the differentiation spectrum – ES cells and the late stages of lineage specification – would call into question its requirement in heritable gene repression mechanisms during cell fate determination. Instead, the facultative heterochromatin marker H3K27me3 is associated with early ES cell bivalent gene expression (Bernstein et al., 2006), and we have detected its presence throughout preimplantation development (Fig. 1A).

To reconcile H4K20me3 in the late differentiated embryo with its presence in self-renewing pluripotent ES cells implies control of the kinetics of histone methyltransferases Suv4-20h1 and Suv4-20h2. These enzymes are already expressed from blastocyst stages (Fig. 1C) and catalyse both dimethylation and trimethylation of H4K20. Wheras early H4K20me3 immunofluorescence signals may be underestimated by the antibody, respective dynamics during development indicate that global dimethylation reaches a plateau long before trimethylation becomes detectable (Fig. 1B). It is possible that trimethylation is a rate-limiting step that occurs only after full dimethylation or, as proposed, that trimethylation specifically requires the recruitment of the Suv4-20h enzymes by HP1 (Schotta et al., 2004). Indeed, we have shown here that HP1α is also present late in development but early in ES cell derivation.

Despite the late onset of its transcription, H4K20me3 is nevertheless an essential epigenetic marker for late foetal development, as demonstrated by the perinatal lethality of the *Suv420h1*/*Suv420h2* knockout mouse (Schotta et al., 2008). This and the observed loss of H4K20me3 mark in cancers (Fraga et al., 2005; Pogribny et al., 2006) seem to support the notion that it is a heterochromatin maintenance marker. Studies in *Drosophila* have reinforced this idea by showing that the H4K20me3 mark, which in this species is not detectable in nuclei until mid-gastrulation (Karachentsev et al., 2007), was sufficient for heritable maintenance of heterochromatin in the absence of other heterochromatin hallmarks (Phalke et al., 2009). In *Xenopus*, histone H4K20me3 was not detected until after gastrulation (Dunican et al., 2008).

Our work concludes that constitutive heterochromatin undergoes very slow changes in composition during embryo to late foetal development, which can also occur rapidly during ES cell derivation. Although its effect on heterochromatin structure and function is as yet unknown, other work suggests that H4K20me3 containing heterochromatin is essential for the maintenance of perinatal, non-cancerous cell states and confers heterochromatin maintenance capability (Fraga et al., 2005; Pogribny et al., 2006; Schotta et al., 2008). We propose that heterochromatin, while contributing to maintaining a cell type by providing a gene-repressive compartment in the nucleus, also retains the dynamics to adapt to sequential cell fate changes during cell lineage specification. As these changes come to an end, a necessary gradual stabilisation follows by increasing the maintenance capabilities of heterochromatin, which relies on the essential acquirement of H4K20me3 and HP1α

Materials and Methods

Animals and embryos

Animal procedures were done in strict accordance with UK Home Office regulations and are covered by a project licence issued under the Animal (Scientific Procedures) Act of 1986. Matings used 6–10 weeks old B6CBAF1 (C57BL/6 × CBA) mice. Zygotes were collected 21 hours post human chorionic gonadotropin (hCG) injection and cultured in vitro as previously described (Ribas et al., 2006). Embryos were collected on day E3.5 and E4.5 by flushing the uterus with 1 ml of M2 medium (Sigma). Embryos at E5.5, E6.5, E7.5, E14.5 and E17.5 were dissected from the uterus. For cryosection, postimplantation embryos (E7.5, E14.5 and E17.5) were placed in OTC reagent (Raymond A Lamb) and immediately frozen on dry ice. Cryosections were cut to 3–5 μm thickness using a cryostat (Leica).

Embryonic stem cells

An established ES cell line (E14tg2a) and early-passage ES-like cells were cultured on either 0.1% gelatine or inactivated mouse embryonic fibroblasts in Dulbecco's modified Eagle's medium (DMEM, Invitrogen) plus 15% foetal bovine serum (FBS), 100 IU/ml leukemia inhibiting factor (LIF) (Chemicon), 100 μM β-mercaptoethanol (Invitrogen), 100 μM non-essential amino acids, 2 mM L-glutamine (Invitrogen) and penicillin–streptomycin (100 IU/ml–100 ug/ml, Sigma) as previously described (Bru et al., 2008). For differentiation assays, ES cells were induced to form embryoid bodies by placing them into a Petri dish (Sterilin) and culturing in DMEM supplemented with 15% FCS at 37°C in a 5% CO_2 incubator. ES cell differentiation was performed according to Nagy et al. (Nagy et al., 2006b). ES cells were also cultured in medium supplemented with serum replacement (SR; KnockOut^{TM}, Invitrogen) for ES derivation experiments.

In vitro implantation

Expanded blastocysts were incubated in ES cell medium on gelatinised chamber slides. After 24 hours, trophectoderm (TE) attached to the plate and differentiated to trophoblast, whereas ICM grew and formed colony-like cells.

Immunofluorescence

Preimplantation embryos (all stages) and postimplantation (E5.5 and E7.5) were stained whole mount, whereas E11.5, E14.5 and E17.5 were cryosectioned and stained. Mouse embryonic fibroblasts were prepared from E14 foetal skin. Immunofluorescence was performed as described previously (Ribas et al., 2006). Briefly, samples were fixed in 4% PFA in PBS at 4°C overnight, permeabilised in 0.2% Triton X-100 (Sigma) for 15–30 minutes, washed twice with 0.01% Tween (Sigma) and then incubated in blocking solution [2% bovine serum albumin (Sigma) or 5% donkey serum (Sigma)] for 2 hours. Samples were incubated with primary antibody either at room temperature for 1 hour or at 4°C overnight (supplementary material Table S1), then washed three times. Samples were then incubated with secondary antibodies that were conjugated with FITC or TRITC (The Jackson Laboratory) using a concentration of 1:200. After the final wash, samples were counterstained with (4′,6-diamidino-2-phenylindole) DAPI in ProLong Gold antifade reagent (Invitrogen).

Microscopy and flow cytometery

Images were captured using a Nikon Ti Eclipse fluorescence microscope and Volocity software (Improvision), or a Zeiss laser confocal microscope (LSM510 Meta) and LSM Meta software. *Z* stack confocal series were obtained at 40× magnification. Merged 3D and 2D images and measurements of fluorescence intensity were

performed using LSM Meta and ImageJ software (Abramoff et al., 2004). Total nuclear fluorescence intensity was calculated by using the mean intensity (30 embryos) multiplied by the average volume of nuclei for each embryo stage. Flow cytometry analysis was performed using a FACScan machine (BD Bioscience). Data were analysed using the program Cell Quest (BD Bioscience).

Protein extraction and western blots

Histone extraction buffer and whole-cell extraction buffer (RIPA) were prepared following a protocol from Upstate Biotech. Protein concentration was measured using the DC protein assay (Bio-Rad). Western blotting was performed using the NuPAGE and XCell systems (Invitrogen) according to manufacturer's instructions. 15 μg of protein was loaded onto each lane of the gel. After the protein transfer step, membranes were blocked with 5% skimmed milk, and then incubated with primary antibodies (supplementary material Table S1) for either 1 hour at room temperature or at 4°C overnight. Membranes were washed five times with 0.1% Tween 20 in PBS for 10 minutes. Thereafter, membranes were incubated with secondary antibodies conjugated with HRP (Amersham). Chemifluorescence was produced by ECL reaction (Amersham) and was detected using X-ray film (Fujifilm) and a Kodak imaging system (Kodak).

Total RNA extraction, cDNA and PCR

Total RNA of 15 embryos was extracted using the RNeasy kit (Qiagen) and concentrated using Pellet Paint® Co-Precipitant (Novagen). cDNA synthesis was performed using a Cloned AMV first-strand synthesis kit (Invitrogen). 2 μl of cDNA (equivalent to 0.1 embryos) was added to Thermostart PCR mix (ABgene). Each step was performed as previously described (Taylor et al., 2009). The PCR products were separated on 1.5% agarose gels. DNA was stained with SYBR gold (Molecular Probes) (1 μl in 100 TBE). DNA bands were observed under UV light and images were captured using a Gel-DOC system (Bio-Rad). A 100-bp DNA ladder (New England Biolab) was used to size the PCR products. Primer sequences were: Suv4-20h1 forward 5′-CACGACAGTGACAGCAACCT-3′, reverse 5′-GTCTGAAGGCCCTATGTGGA-3′; Suv4-20h2 forward 5′-TGCGTGAAGAGGATGAAGAC-3′, reverse 5′-TAGGCGGGTAAGTTCCACAC-3′; Gapdh forward 5′-AACAACCCCTTCATTGACCTC-3′, reverse 5′-TTCTGAGTGGCAGTGATGGC-3′.

Statistics

All statistics was carried out using SPSS 14 software. Significant differences in fluorescence intensity were calculated using GLM and Student's *t*-test. Statistical differences between E14.5 and E17.5 were calculated using χ^2 with SPSS 14 software.

We thank Busabun Wongtawan for assistance with western blot analysis, and Richard Meehan, Gunnar Schotta and Thomas Theil for experimental suggestions and discussions. This research was funded by a Thai Royal Studentship-Office of the Higher Education Commission to T.W. and BBSRC grant BB/E023355 to S.P., I.W. and J.E.T. Deposited in PMC for release after 6 months.

Supplementary material available online at
http://jcs.biologists.org/cgi/content/full/124/11/1878/DC1

References

Abramoff, M. D., Magelhaes, P. J. and Ram, S. J. (2004). Image processing with ImageJ. *Biophotonics Int.* **11**, 36-42.

Ayoub, N., Jeyasekharan, A. D., Bernal, J. A. and Venkitaraman, A. R. (2008). HP1-beta mobilization promotes chromatin changes that initiate the DNA damage response. *Nature* **453**, 682-686.

Barski, A., Cuddapah, S., Cui, K., Roh, T. Y., Schones, D. E., Wang, Z., Wei, G., Chepelev, I. and Zhao, K. (2007). High-resolution profiling of histone methylations in the human genome. *Cell*. **129**, 823-837.

Benetti, R., Gonzalo, S., Jaco, I., Schotta, G., Klatt, P., Jenuwein, T. and Blasco, M. A. (2007). Suv4-20h deficiency results in telomere elongation and derepression of telomere recombination. *J. Cell Biol*. **178**, 925-936.

Bernstein, B. E., Mikkelsen, T. S., Xie, X., Kamal, M., Huebert, D. J., Cuff, J., Fry, B., Meissner, A., Wernig, M., Plath, K. et al. (2006). A bivalent chromatin structure marks key developmental genes in embryonic stem cells. *Cell* **125**, 315-326.

Biron, V. L., McManus, K. J., Hu, N., Hendzel, M. J. and Underhill, D. A. (2004). Distinct dynamics and distribution of histone methyl-lysine derivatives in mouse development. *Dev. Biol*. **276**, 337-351.

Bongiorni, S., Pasqualini, B., Taranta, M., Singh, P. B. and Prantera, G. (2007). Epigenetic regulation of facultative heterochromatinisation in Planococcus citri via the Me(3)K9H3-HP1-Me(3)K20H4 pathway. *J. Cell Sci.* **120**, 1072-1080.

Bru, T., Clarke, C., McGrew, M. J., Sang, H. M., Wilmut, I. and Blow, J. J. (2008). Rapid induction of pluripotency genes after exposure of human somatic cells to mouse ES cell extracts. *Exp. Cell Res*. **314**, 2634-2642.

Chambers, I., Silva, J., Colby, D., Nichols, J., Nijmeijer, B., Robertson, M., Vrana, J., Jones, K., Grotewold, L. and Smith, A. (2007). Nanog safeguards pluripotency and mediates germline development. *Nature* **450**, 1230-1234.

Clark, A. T., Bodnar, M. S., Fox, M., Rodriquez, R. T., Abeyta, M. J., Firpo, M. T. and Pera, R. A. (2004). Spontaneous differentiation of germ cells from human embryonic stem cells in vitro. *Hum. Mol. Genet*. **13**, 727-739.

Creyghton, M. P., Markoulaki, S., Levine, S. S., Hanna, J., Lodato, M. A., Sha, K., Young, R. A., Jaenisch, R. and Boyer, L. A. (2008). H2AZ is enriched at polycomb complex target genes in ES cells and is necessary for lineage commitment. *Cell* **135**, 649-661.

Dahl, J. A., Reiner, A. H., Klungland, A., Wakayama, T. and Collas, P. (2010). Histone H3 lysine 27 methylation asymmetry on developmentally-regulated promoters distinguish the first two lineages in mouse preimplantation embryos. *PLoS ONE* **5**, e9150.

Daujat, S., Weiss, T., Mohn, F., Lange, U. C., Ziegler-Birling, C., Zeissler, U., Lappe, M., Schubeler, D., Torres-Padilla, M. E. and Schneider, R. (2009). H3K64 trimethylation marks heterochromatin and is dynamically remodeled during developmental reprogramming. *Nat. Struct. Mol. Biol*. **16**, 777-781.

Dawson, M. A., Bannister, A. J., Göttgens, B., Foster, S. D., Bartke, T., Green, A. R. and Kouzarides, T. (2009). JAK2 phosphorylates histone H3Y41 and excludes HP1alpha from chromatin. *Nature* **461**, 819-822.

Delaval, K., Govin, J., Cerqueira, F., Rousseaux, S., Khochbin, S. and Feil, R. (2007). Differential histone modifications mark mouse imprinting control regions during spermatogenesis. *EMBO J*. **26**, 720-729.

Dialynas, G. K., Terjung, S., Brown, J. P., Aucott, R. L., Baron-Luhr, B., Singh, P. B. and Georgatos, S. D. (2007). Plasticity of HP1 proteins in mammalian cells. *J. Cell Sci.* **120**, 3415-3424.

Dillon, N. (2004). Heterochromatin structure and function. *Biol. Cell* **96**, 631-637.

Dunican, D. S., Ruzov, A., Hackett, J. A. and Meehan R. R. (2008). xDnmt1 regulates transcriptional silencing in pre-MBT Xenopus embryos independently of its catalytic function. *Development* **135**, 1295-1302.

Efroni, S., Duttagupta, R., Cheng, J., Dehghani, H., Hoeppner, D. J., Dash, C., Bazett-Jones, D. P., Le Grice, S., McKay, R. D., Buetow, K. H. et al. (2008). Global transcription in pluripotent embryonic stem cells. *Cell Stem Cell* **2**, 437-447.

Fanti, L. and Pimpinelli, S. (2008). HP1: a functionally multifaceted protein. *Curr. Opin. Genet. Dev*. **18**, 169-174.

Fedorova, E. and Zink, D. (2008). Nuclear architecture and gene regulation. *Biochim. Biophys. Acta* **1783**, 2174-2184.

Fraga, M. F., Ballestar, E., Villar-Garea, A., Boix-Chornet, M., Espada, J., Schotta, G., Bonaldi, T., Haydon, C., Ropero, S., Petrie, K. et al. (2005). Loss of acetylation at Lys16 and trimethylation at Lys20 of histone H4 is a common hallmark of human cancer. *Nat. Genet*. **37**, 391-400.

Furusawa, T., Ikeda, M., Inoue, F., Ohkoshi, K., Hamano, T. and Tokunaga, T. (2006). Gene expression profiling of mouse embryonic stem cell subpopulations. *Biol. Reprod*. **75**, 555-561.

Gartenberg, M. (2009). Heterochromatin and the cohesion of sister chromatids. *Chromosome Res*. **17**, 229-238.

Gilbert, N., Boyle, S., Sutherland, H., de Las Heras, J., Allan, J., Jenuwein, T. and Bickmore, W. A. (2003). Formation of facultative heterochromatin in the absence of HP1. *EMBO J*. **22**, 5540-5550.

Grewal, S. I. and Jia, S. (2007). Heterochromatin revisited. *Nat. Rev. Genet*. **8**, 35-46.

Griffiths, D. S., Li, J., Dawson, M. A., Trotter, M. W., Cheng, Y. H., Smith, A. M., Mansfield, W., Liu, P., Kouzarides, T., Nichols, J. et al. (2011). LIF-independent JAK signalling to chromatin in embryonic stem cells uncovered from an adult stem cell disease. *Nat. Cell Biol.* **13**, 13-21.

Hemberger, M. (2007). Epigenetic landscape required for placental development. *Cell. Mol. Life Sci*. **64**, 2422-2436.

Horie, K., Takakura, K., Taii, S., Narimoto, K., Noda, Y., Nishikawa, S., Nakayama, H., Fujita, J. and Mori, T. (1991). The expression of c-kit protein during oogenesis and early embryonic development. *Biol. Reprod*. **45**, 547-552.

Houlard, M., Berlivet, S., Probst, A. V., Quivy, J. P., Hery, P., Almouzni, G. and Gerard, M. (2006). CAF-1 is essential for heterochromatin organization in pluripotent embryonic cells. *PLoS Genet*. **2**, e181.

Karachentsev, D., Druzhinina, M. and Steward, R. (2007). Free and chromatin-associated mono-, di- and trimethylation of histone H4-lysine 20 during development and cell cycle progression. *Dev. Biol*. **304**, 46-52.

Kobayakawa, S., Miike, K., Nakao, M. and Abe, K. (2007). Dynamic changes in the epigenomic state and nuclear organization of differentiating mouse embryonic stem cells. *Genes Cells* **12**, 447-460.

Kourmouli, N., Jeppesen, P., Mahadevhaiah, S., Burgoyne, P., Wu, R., Gilbert, D. M., Bongiorni, S., Prantera, G., Fanti, L., Pimpinelli, S. et al. (2004). Heterochromatin and tri-methylated lysine 20 of histone H4 in animals. *J. Cell Sci.* **117**, 2491-2501.

Kourmouli, N., Sun, Y. M., van der Sar, S., Singh, P. B. and Brown, J. P. (2005). Epigenetic regulation of mammalian pericentric heterochromatin in vivo by HP1. *Biochem. Biophys. Res. Commun*. **337**, 901-907.

Lee, J., Thompson, J. R., Botuyan, M. V. and Mer, G. (2008). Distinct binding modes specify the recognition of methylated histones H3K4 and H4K20 by JMJD2A-tudor. *Nat. Struct. Mol. Biol*. **15**, 109-111.

Lehnertz, B., Ueda, Y., Derijck, A. A., Braunschweig, U., Perez-Burgos, L., Kubicek, S., Chen, T., Li, E., Jenuwein, T. and Peters, A. H. (2003). Suv39h-mediated histone H3 lysine 9 methylation directs DNA methylation to major satellite repeats at pericentric heterochromatin. *Curr. Biol*. **13**, 1192-1200.

Li, W. X. (2008). Canonical and non-canonical JAK-STAT signaling. *Trends Cell Biol.* **18**, 545-551.

Martens, J. H., O'Sullivan, R. J., Braunschweig, U., Opravil, S., Radolf, M., Steinlein, P. and Jenuwein, T. (2005). The profile of repeat-associated histone lysine methylation states in the mouse epigenome. *EMBO J*. **24**, 800-812.

Martin, C., Beaujean, N., Brochard, V., Audouard, C., Zink, D. and Debey, P. (2006). Genome restructuring in mouse embryos during reprogramming and early development. *Dev. Biol*. **292**, 317-332.

Meehan, R. R., Dunican, D. S., Ruzov, A. and Pennings, S. (2005). Epigenetic silencing in embryogenesis. *Exp. Cell Res*. **309**, 241-249.

Meshorer, E., Yellajoshula, D., George, E., Scambler, P. J., Brown, D. T. and Misteli, T. (2006). Hyperdynamic plasticity of chromatin proteins in pluripotent embryonic stem cells. *Dev. Cell* **10**, 105-116.

Nagy, A., Gertsenstein, M., Vintersten, K. and Behringer, R. (2006a). De novo isolation of embryonic stem (ES) cell lines from blastocysts. *Cold Spring Harb. Protoc.* **1**, doi: 10.1101/pdb.prot4403.

Nagy, A., Gertsenstein, M., Vintersten, K. and Behringer, R. (2006b). Differentiating embryonic stem (ES) cells into embryoid bodies. *Cold Spring Harb. Protoc.* **2**, doi: 10.1101/pdb.prot4405.

Nishi, O., Tominaga, T., Goto, Y., Hayashi, K. and Mori, T. (1995). Effects of platelet activating factor on mouse embryo implantation in vitro. *J. Assist. Reprod. Genet*. **12**, 330-334.

Pannetier, M., Julien, E., Schotta, G., Tardat, M., Sardet, C., Jenuwein, T. and Feil, R. (2008). PR-SET7 and SUV4-20H regulate H4 lysine-20 methylation at imprinting control regions in the mouse. *EMBO Rep*. **9**, 998-1005.

Peters, A. H., Mermoud, J. E., O'Carroll, D., Pagani, M., Schweizer, D., Brockdorff, N. and Jenuwein, T. (2002). Histone H3 lysine 9 methylation is an epigenetic imprint of facultative heterochromatin. *Nat. Genet*. **30**, 77-80.

Phalke, S., Nickel, O., Walluscheck, D., Hortig, F., Onorati, M. C. and Reuter, G. (2009). Retrotransposon silencing and telomere integrity in somatic cells of Drosophila depends on the cytosine-5 methyltransferase DNMT2. *Nat. Genet*. **41**, 696-702.

Pogribny, I. P., Ross, S. A., Tryndyak, V. P., Pogribna, M., Poirier, L. A. and Karpinets, T. V. (2006). Histone H3 lysine 9 and H4 lysine 20 trimethylation and the expression of Suv4-20h2 and Suv-39h1 histone methyltransferases in hepatocarcinogenesis induced by methyl deficiency in rats. *Carcinogenesis* **27**, 1180-1186.

Probst, A. V., Santos, F., Reik, W., Almouzni, G. and Dean, W. (2007). Structural differences in centromeric heterochromatin are spatially reconciled on fertilisation in the mouse zygote. *Chromosoma* **116**, 403-415.

Quinn, J., Kunath, T. and Rossant, J. (2006). Mouse trophoblast stem cells. *Methods Mol. Med*. **121**, 125-148.

Rangasamy, D., Berven, L., Ridgway, P. and Tremethick, D. J. (2003). Pericentric heterochromatin becomes enriched with H2A.Z during early mammalian development. *EMBO J*. **22**, 1599-1607.

Regha, K., Sloane, M. A., Huang, R., Pauler, F. M., Warczok, K. E., Melikant, B., Radolf, M., Martens, J. H., Schotta, G., Jenuwein, T. et al. (2007). Active and repressive chromatin are interspersed without spreading in an imprinted gene cluster in the mammalian genome. *Mol. Cell* **27**, 353-366.

Reijo Pera, R. A., DeJonge, C., Bossert, N., Yao, M., Hwa Yang, J. Y., Asadi, N. B., Wong, W., Wong, C. and Firpo, M. T. (2009). Gene expression profiles of human inner cell mass cells and embryonic stem cells. *Differentiation* **78**, 18-23.

Ribas, R. C., Taylor, J. E., McCorquodale, C., Mauricio, A. C., Sousa, M. and Wilmut, I. (2006). Effect of zona pellucida removal on DNA methylation in early mouse embryos. *Biol. Reprod*. **74**, 307-313.

Sarg, B., Koutzamani, E., Helliger, W., Rundquist, I. and Lindner, H. H. (2002). Postsynthetic trimethylation of histone H4 at lysine 20 in mammalian tissues is associated with aging. *J. Biol. Chem*. **277**, 39195-39201.

Schones, D. E. and Zhao, K. (2008). Genome-wide approaches to studying chromatin modifications. *Nat. Rev. Genet*. **9**, 179-191.

Schotta, G., Lachner, M., Sarma, K., Ebert, A., Sengupta, R., Reuter, G., Reinberg, D. and Jenuwein, T. (2004). A silencing pathway to induce H3-K9 and H4-K20 trimethylation at constitutive heterochromatin. *Genes Dev*. **18**, 1251-1262.

Schotta, G., Sengupta, R., Kubicek, S., Malin, S., Kauer, M., Callen, E., Celeste, A., Pagani, M., Opravil, S., De La Rosa-Velazquez, I. A. et al. (2008). A chromatin-wide transition to H4K20 monomethylation impairs genome integrity and programmed DNA rearrangements in the mouse. *Genes Dev*. **22**, 2048-2061.

Shumaker, D. K., Dechat, T., Kohlmaier, A., Adam, S. A., Bozovsky, M. R., Erdos, M. R., Eriksson, M., Goldman, A. E., Khuon, S., Collins, F. S. et al. (2006). Mutant nuclear lamin A leads to progressive alterations of epigenetic control in premature aging. *Proc. Natl. Acad. Sci. USA* **103**, 8703-8708.

Singh, A. M., Hamazaki, T., Hankowski, K. E. and Terada, N. (2007). A heterogeneous expression pattern for Nanog in embryonic stem cells. *Stem Cells* **25**, 2534-2542.

Stadler, F., Kolb, G., Rubusch, L., Baker, S. P., Jones, E. G. and Akbarian, S. (2005). Histone methylation at gene promoters is associated with developmental regulation and region-specific expression of ionotropic and metabotropic glutamate receptors in human brain. *J. Neurochem*. **94**, 324-336.

Tang, F., Barbacioru, C., Bao, S., Lee, C., Nordman, E., Wang, X., Lao, K. and Surani, M. A. (2010). Tracing the derivation of embryonic stem cells from the inner cell mass by single-cell RNA-seq analysis. *Cell Stem Cell* **6**, 468-478.

Taylor, J., Moore, H., Beaujean, N., Gardner, J., Wilmut, I., Meehan, R. and Young, L. (2009). Cloning and expression of sheep DNA methyltransferase 1 and its development-specific isoform. *Mol. Reprod. Dev*. **76**, 501-513.

Toyooka, Y., Tsunekawa, N., Akasu, R. and Noce, T. (2003). Embryonic stem cells can form germ cells in vitro. *Proc. Natl. Acad. Sci. USA* **100**, 11457-11462.

Toyooka, Y., Shimosato, D., Murakami, K., Takahashi, K. and Niwa, H. (2008). Identification and characterization of subpopulations in undifferentiated ES cell culture. *Development* **135**, 909-918.

van der Heijden, G. W., Dieker, J. W., Derijck, A. A., Muller, S., Berden, J. H., Braat, D. D., van der Vlag, J. and de Boer, P. (2005). Asymmetry in histone H3 variants and lysine methylation between paternal and maternal chromatin of the early mouse zygote. *Mech. Dev*. **122**, 1008-1022.

Wang, G., Zhou, D., Wang, C., Gao, Y., Zhou, Q., Qian, G. and DeCoster, M. A. (2010). Hypoxic preconditioning suppresses group III secreted phospholipase A2-induced apoptosis via JAK2-STAT3 activation in cortical neurons. *J. Neurochem.* **114**, 1039-1048.

Ying, Q. L., Wray, J., Nichols, J., Batlle-Morera, L., Doble, B., Woodgett, J., Cohen, P. and Smith, A. (2008). The ground state of embryonic stem cell self-renewal. *Nature* **453**, 519-523.